

Two cases of pulmonary paragonimiasis on FDG-PET CT imaging

Je Ryung YOO, Hyun Jin PARK, Joo HYUN O, Yong An CHUNG,
Hyung Sun SOHN, Soo Kyo CHUNG and Sung Hoon KIM

*Department of Radiology, The Catholic University of Korea, College of Medicine,
Kangnam St. Mary's Hospital, Seoul, Republic of Korea*

Positron emission tomography (PET) using ^{18}F -fluorodeoxyglucose (FDG) is useful in cancer diagnosis owing to its sensitivity to the differences in glucose metabolic rate between benign and malignant diseases, especially in the lung. One pitfall in PET imaging of lung disease, however, is the overlap in metabolic rate of inflammatory and neoplastic entities. Paragonimiasis is a food-borne parasitic disease that causes the pulmonary and pleural inflammation. We present two cases of pulmonary paragonimiasis that showed high uptake suggestive of tumor on FDG-PET CT images, both confirmed on histopathology by visualization of *Paragonimus westermani* eggs in the involved tissues.

Key words: paragonimiasis, *Paragonimus westermani*, lung, positron-emission tomography

CASE REPORT

PET using ^{18}F -FDG is frequently used to characterize pulmonary lesions suspicious for malignancy. However, increased ^{18}F -FDG uptake in benign pulmonary lesions is not uncommon, and can be seen in active granulomatous diseases such as tuberculosis, fungal infection, sarcoidosis, and other inflammatory entities. Paragonimiasis is a relatively rare cause of pulmonary disease; there have been only a few reported cases of pulmonary paragonimiasis as a cause of false-positive results on FDG-PET examinations. We have found two cases of pulmonary paragonimiasis which were false-positive for malignancy on FDG-PET CT scan.

Case 1

A 49-year-old man was referred to us from a local clinic in June 2004 for left upper quadrant abdominal pain and a solitary pulmonary nodule (SPN) in the left lung. The patient had a 30 pack-year smoking history. Routine

laboratory tests were positive only for a mild eosinophilia of 8.4% (normal, less than 5%). Blood and urine cultures, as well as sputum cultures for bacteria and acid-fast organisms, were negative. Chest X-ray showed a patchy left upper lobe opacity near the aortic arch. Chest CT (Fig. 1) showed a 28 mm \times 26 mm irregular cavitory nodule in the anterior segment of the left upper lobe, and several enlarged mediastinal nodes adjacent to the aortic arch. FDG-PET CT (Biograph LSO: Siemens Medical Solutions, Knoxville, Tenn.) demonstrated FDG uptake with a SUV of 4.0 in the cavitory lesion, and slightly increased uptake in the mediastinal lymph nodes (Fig. 2a, b). Because inflammatory uptake tends to decrease and malignant uptake tends to increase over time, two-hour delayed images were subsequently obtained. The peak SUV of the cavitory lesion at 2 hours was 4.1, an insignificant increase of 2.5%.

The patient was transferred to the department of thoracic surgery for open lung biopsy, and then underwent a left upper lobe segmentectomy. The pathologic diagnosis from both frozen and permanent sections was paragonimiasis. Microscopic images (Fig. 3) showed eggs of *Paragonimus westermani* (arrowheads) surrounded by chronic inflammation and fibrosis.

Case 2

A 56-year-old man was referred from a local clinic in April 2004 with a one-month history of blood-tinged

Received October 11, 2005, revision accepted January 6, 2006.

For reprint contact: Sung Hoon Kim, M.D., Department of Radiology, Kangnam St. Mary's Hospital, The Catholic University of Korea, Seocho-gu, Banpo-dong, #505, Seoul, 137-040, Republic of Korea.

E-mail: sghnk@catholic.ac.kr



Fig. 1 A 49-year-old man presenting with left upper quadrant abdominal pain and SPN of the left lung in June 2004. Chest CT depicted an irregular cavitary nodule in the anterior segment of left upper lobe (*arrow*), and a few enlarged mediastinal nodes adjacent to the aortic arch (*short arrow*).

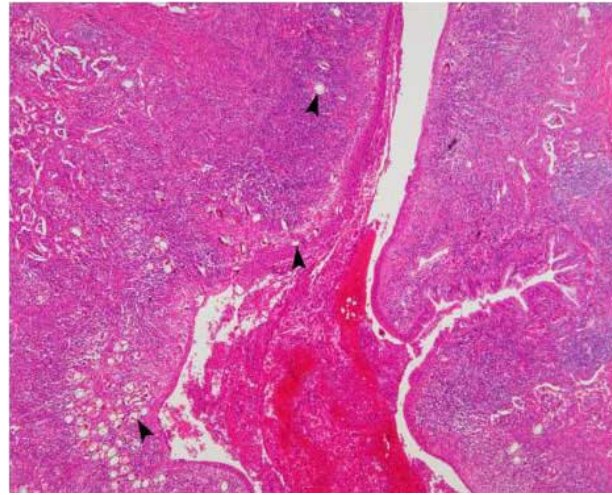
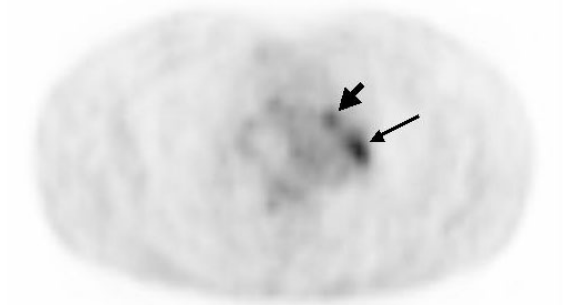
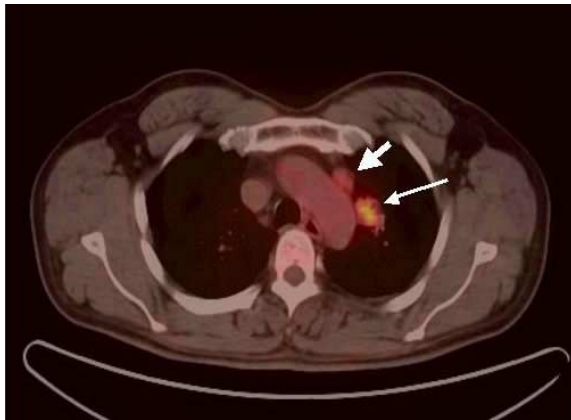


Fig. 3 Photomicrograph (H&E, $\times 40$) reveals operculated, oval yellowish colored eggs of *Paragonimus westermani* (*arrow-heads*), surrounded by chronic inflammation and fibrosis. Bronchial mucosa is eroded.

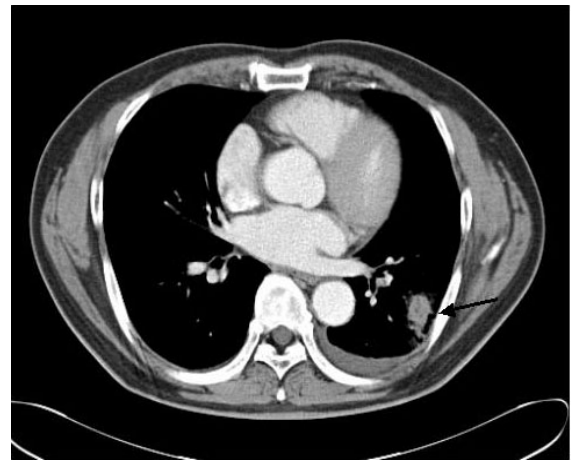


a



b

Fig. 2 Axial PET (a) and axial PET CT fusion (b) images demonstrated moderately increased FDG uptake in the cavitary lesion of the left upper lobe (*arrows*), and mild FDG activity in enlarged lymph nodes in the paraaortic nodal station (*short arrows*).



a



b

Fig. 4 A 56-year-old man presenting with blood tinged sputum during 1 month in April 2004. Chest CT (a&b) demonstrated an irregular nodule with a tiny cavity and surrounding ground-glass opacity in the left lower lobe (*arrow*), and enlarged left hilar adenopathy (*short arrow*). Small amount of fluid collection was noted.

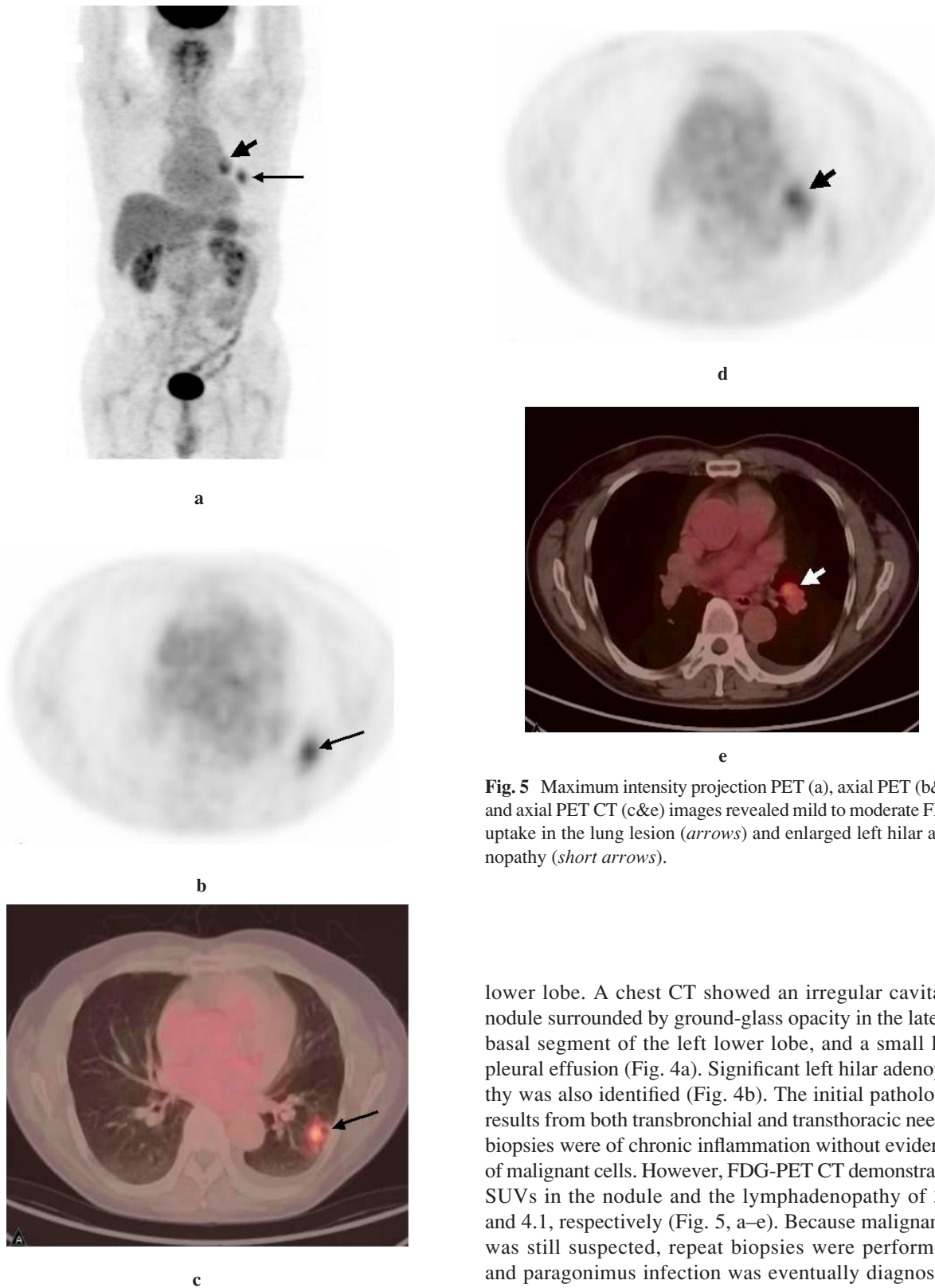


Fig. 5 Maximum intensity projection PET (a), axial PET (b&d) and axial PET CT (c&e) images revealed mild to moderate FDG uptake in the lung lesion (*arrows*) and enlarged left hilar adenopathy (*short arrows*).

sputum. Routine laboratory results, including examination for bacteria and acid-fast organisms, were nonspecific except for an elevated eosinophil count of 12.3%. Chest X-ray showed ill-defined consolidation in the left

lower lobe. A chest CT showed an irregular cavitory nodule surrounded by ground-glass opacity in the lateral basal segment of the left lower lobe, and a small left pleural effusion (Fig. 4a). Significant left hilar adenopathy was also identified (Fig. 4b). The initial pathologic results from both transbronchial and transthoracic needle biopsies were of chronic inflammation without evidence of malignant cells. However, FDG-PET CT demonstrated SUVs in the nodule and the lymphadenopathy of 3.9 and 4.1, respectively (Fig. 5, a–e). Because malignancy was still suspected, repeat biopsies were performed, and paragonimus infection was eventually diagnosed. The patient began praziquantel therapy, and a follow-up chest CT performed 2 weeks later showed a marked diminution in size of the nodule with thinning of the cavity walls (Fig. 6).

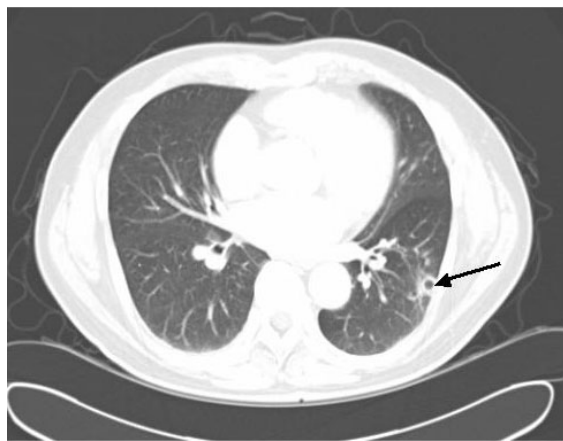


Fig. 6 Two weeks follow-up chest CT depicted markedly diminished size of the nodule with thinning of the cavity walls (arrow).

DISCUSSION

PET using FDG is highly accurate in evaluating pulmonary lesions, aiding in the noninvasive preoperative staging of lung cancer in the past decade.^{1,2} Although nodules less than 1 cm cannot be evaluated accurately, the overall sensitivity and specificity of FDG-PET for the diagnosis of pulmonary lesions are high.³ FDG-PET imaging takes advantage of the higher metabolic rate of tumor cells to show increased accumulation of FDG in malignant lesions. However, an increased metabolic rate is also observed in inflammation.⁴ Many reports have demonstrated increased FDG uptake in inflammatory, infectious and granulomatous lung diseases including parasite infestations, bacterial, and fungal infections, and tuberculosis.^{5–13}

In a recent meta-analysis by Could et al.,¹ the estimated sensitivity of PET for identifying lung malignancies is 96.8% and its specificity is 77.8%. It is well known that most lung malignancies have a greater uptake of FDG than normal tissue. Of the various cutoff values, a threshold for a single time point SUV of 2.5–3.8 has been recommended as the optimal threshold for differentiating benign from malignant pulmonary lesions, despite considerable overlap of benign and malignant in this range.^{14–16}

Recently, scanners combining functional and anatomical modalities have been developed. Of these, use of PET CT has rapidly increased worldwide. It offers significant advantages in localizing FDG uptake, distinguishing pathologic from physiologic uptake, and monitoring disease progression. Especially in non-small cell lung cancer, PET CT has proven to be superior over PET alone or CT alone in disease staging.¹⁷ We use PET CT scanning routinely in our hospital.

Zhuang et al.¹⁸ reported that dual-time-point FDG-PET may be useful in distinguishing benign from malignant

lesions by exploiting the early peak and early washout FDG from inflammatory tissues. Kubota et al.¹⁹ showed improved per-patient sensitivity from 78% with imaging at 1 hour to 94% with imaging at 2 hours. Matthies et al.²⁰ reported that dual-time-point scanning with a threshold value of 10% increase from 70 min to 123 min achieved a sensitivity of 100% with a specificity of 89%. In one of our cases, the uptake increased by only 2.5% between the two time points, suggesting benignity.

Despite the above mentioned efforts, the specificity of FDG-PET is still lower in geographic regions with a high prevalence of granulomatous disease due to an increased rate of false positives. Goo et al.⁵ reported that 9 of 10 tuberculomas demonstrated FDG uptake with a mean peak SUV of 4.2 ± 2.2 . Croft et al.⁶ concluded that the low specificity of their results in differentiating non-small cell lung cancer from benign SPNs might be related to a high endemic rate of histoplasmosis.

Paragonimiasis is a food-borne parasitic disease common in Southeast Asia, especially in Japan, Korea, the Philippines, Taiwan, and parts of China. The high endemic rates of paragonimiasis are related to dietary habits and methods of food preparation common to these areas. The radiologic findings of this parasite infestation when it involves the lung are quite variable, making diagnosis difficult with imaging alone. Diagnosis begins with a thorough history, and the operculated eggs of *Paragonimus* in sputum is the most specific indicator of the disease. Alternatively, if the clinical history is suspicious but the sputum negative for eggs, the diagnosis can be made with an enzyme-linked immunosorbent assay (ELISA).^{7,21,22} Therefore, we suggest that in the setting of a patient with a lung lesion with equivocal imaging findings, a history of handling and/or eating freshwater crab or crayfish in an endemic area, and eosinophilia, parasitic disease needs to be included in the differential diagnosis.

In conclusion, positive results on an FDG-PET scan must be interpreted with caution in geographic regions with high prevalences of parasites, tuberculosis, and fungal disease.

REFERENCES

1. Could MK, Maclean CC, Kuschner WG, Rydzak CE, Owens DK. Accuracy of positron emission tomography for diagnosis of pulmonary nodules and mass lesions. *JAMA* 2001; 285: 914–924.
2. Kelly RK, Tran T, Holmstrom A, Murar J, Segurolo RJ Jr. Accuracy and cost-effectiveness of [¹⁸F]-2-fluoro-deoxy-D-glucose positron emission tomography scan in potentially resectable non-small cell lung cancer. *Chest* 2004; 125: 1413–1423.
3. Nomori H, Watanabe K, Ohtsuka T, Naruke T, Suemasu K, Uno K. Evaluation of F-18 fluorodeoxyglucose (FDG) PET scanning for pulmonary nodules less than 3 cm in diameter, with special reference to the CT images. *Lung Cancer* 2004; 45: 19–27.

4. Imdahl A, Jenkner S, Brink I, Nitzsche E, Stoelben E, Moser E, et al. Validation of FDG positron emission tomography for differentiation of unknown pulmonary lesions. *Eur J Cardiothorac Surg* 2001; 20: 324–329.
5. Goo JM, Im JG, Do KH, Yeo JS, Seo JB, Kim HY, et al. Pulmonary tuberculoma evaluated by means of FDG PET: findings in 10 cases. *Radiology* 2000; 216: 117–121.
6. Croft DR, Trapp J, Kernstine K, Kirchner P, Mullan B, Galvin J, et al. FDG-PET imaging and the diagnosis of non-small cell lung cancer in a region of high histoplasmosis prevalence. *Lung Cancer* 2002; 36: 297–301.
7. Watanabe S, Nakamura Y, Kariatsumari K, Nagata T, Sakata R, Zinnouchi S, et al. Pulmonary paragonimiasis mimicking lung cancer on FDG-PET imaging. *Anticancer Res* 2003; 23: 3437–3440.
8. Zhuang H, Duarte PS, Rebenstock A, Feng Q, Alavi A. Pulmonary clostridium perfringens infection detected by FDG positron emission tomography. *Clin Nucl Med* 2003; 28: 517–518.
9. Hsu CH, Lee CM, Wang FC, Lin YH. F-18 fluorodeoxyglucose positron emission tomography in pulmonary cryptococcoma. *Clin Nucl Med* 2003; 28: 791–793.
10. Wilkinson MD, Fulham MJ, McCaughan BC, Constable CJ. Invasive aspergillosis mimicking stage IIIA non-small-cell lung cancer on FDG positron emission tomography. *Clin Nucl Med* 2003; 28: 234–235.
11. Beggs AD, Hain SF. F-18 FDG-positron emission tomographic scanning and Wegener's granulomatosis. *Clin Nucl Med* 2002; 27: 705–706.
12. Talwar A, Mayerhoff R, London D, Shah R, Stanek A, Epstein M. False-positive PET scan in a patient with lipoid pneumonia simulating lung cancer. *Clin Nucl Med* 2004; 29: 426–428.
13. Kao CH, Tsai SC, Hung GU. Two incorrect FDG positron emission tomography interpretations of a pulmonary mass and mediastinal lymphadenopathy. *Clin Nucl Med* 2001; 26: 1049–1050.
14. Patz EF Jr, Lowe VJ, Hoffman JM, Paine SS, Burrowes P, Coleman RE, et al. Focal pulmonary abnormalities: evaluation with F-18 fluorodeoxyglucose PET scanning. *Radiology* 1993; 188: 487–490.
15. Hubner KF, Buonocore E, Gould HR, Thie J, Smith GT, Stephens S, et al. Differentiating benign from malignant lung lesions using "quantitative" parameters of FDG PET images. *Clin Nucl Med* 1996; 21: 941–949.
16. Yang SN, Liang JA, Lin FJ, Kwan AS, Kao CH, Shen YY. Differentiating benign and malignant pulmonary lesions with FDG-PET. *Anticancer Res* 2001; 21: 4153–4157.
17. Schillaci O, Simonetti G. Fusion imaging in nuclear medicine-application of dual-modality systems in oncology. *Cancer Biother Radiopharm* 2004; 19: 1–10.
18. Zhuang H, Pourdehnad M, Lambright ES, Yamamoto AJ, Lanuti M, Li P, et al. Dual time point ¹⁸F-FDG PET imaging for differentiating malignant from inflammatory processes. *J Nucl Med* 2001; 42: 1412–1417.
19. Kubota K, Itoh M, Ozaki K, Ono S, Tashiro M, Yamaguchi K, et al. Advantage of delayed whole-body FDG-PET imaging for tumour detection. *Eur J Nucl Med* 2001; 28: 696–703.
20. Matthies A, Hickeys M, Cuchiara A, Alavi A. Dual time point ¹⁸F-FDG PET for the evaluation of pulmonary nodules. *J Nucl Med* 2002; 43: 871–875.
21. Mukae H, Taniguchi H, Matsumoto N, Iiboshi H, Ashitani J, Matsukura S, et al. Clinicoradiologic features of pleuropulmonary *Paragonimus westermani* on Kyusyu Island, Japan. *Chest* 2001; 120: 514–520.
22. DeFrain M, Hooker R. North American paragonimiasis, case report of a severe clinical infection. *Chest* 2002; 121: 1368–1372.